Unlocking corrosion defense: investigating Schiff base derivatives for enhanced mild steel protection in acidic environments

I.A. Annon,[1] K.K. Jlood,[1] N. Betti,[2] T.S. Gaaz,[3] M.M. Hanoon,[1] F.F. Sayyid,[1] A.M. Mustafa[1] and A.A. Alamiery[4,5]*

[1]*Department of Production Engineering and Metallurgical, University of Technology, Baghdad P.O. Box 10001, Iraq*
[2]*Materials Engineering Department, University of Technology-Iraq, Baghdad 10001, Iraq*
[3]*Air Conditioning and Refrigeration Techniques Engineering Department, College of Engineering and Technologies, Al-Mustaqbal University, Babylon 51001, Iraq*
[4]*University of Technology, Baghdad P.O. Box 10001, Iraq*
[5]*University Kebangsaan Malaysia, Bangi P.O. Box 43000, Selangor, Malaysia*
**E-mail: dr.ahmed1975@gmail.com*

Abstract

This study explores the potential of a compound named 1-(2,4,6-trihydroxyphenyl)ethanone thiosemicarbazone (TET) to protect mild steel from rusting in a harsh acidic environment (hydrochloric acid). We tested how well TET performs at different temperatures and exposure times. The results show that TET can be highly effective in preventing corrosion, achieving a maximum protection of almost 90%. Interestingly, its effectiveness increases as you add more TET, but decreases slightly at higher temperatures. Further analysis suggests that TET forms a protective layer on the steel surface. To understand this process better, we used computer modeling to examine the molecule's structure and properties. This analysis revealed factors that contribute to TET's ability to inhibit corrosion. Overall, this research provides valuable insights into TET's potential as a corrosion inhibitor. It paves the way for designing even more effective and environmentally friendly solutions to protect metals from rust.

Received: January 3, 2024. Published: April 16, 2024 doi: 10.17675/2305-6894-2024-13-2-5

Keywords: *corrosion inhibitor, density functional theory, Schiff base, Langmuir adsorption isotherm, mild steel alloy.*

1. Introduction

Corrosion of metallic materials is a pervasive and economically significant phenomenon, particularly in aggressive environments such as hydrochloric acid (HCl) solutions [1–5]. The deleterious effects of corrosion on infrastructure, industrial equipment, and various metal alloys necessitate the development of effective corrosion inhibitors to mitigate the economic and safety concerns associated with material degradation [6–8]. In this context, organic compounds, especially Schiff bases, have garnered considerable attention as corrosion inhibitors due to their versatile chemical structures and promising inhibitive

properties [9–12]. Schiff bases are organic compounds derived from the condensation reaction between a primary amine and a carbonyl compound. These compounds are renowned for their wide array of applications in medicinal chemistry, coordination chemistry, and, pertinent to this study, corrosion inhibition. The ability of bases to form complex structures with metal ions and their potential for adsorption onto metal surfaces make them intriguing candidates for corrosion inhibition studies [13–22]. One such Schiff base, 1-(2,4,6-trihydroxyphenyl)ethanone thiosemicarbazone (TET), has emerged as a compelling corrosion inhibitor for mild steel alloy in HCl environments. TET presents a unique molecular structure that combines the reactivity of carbonyl and thiosemicarbazone moieties, potentially facilitating strong interactions with metal surfaces. The incorporation of hydroxyl groups in the phenyl ring further enhances the adsorption capabilities of TET, making it a promising candidate for corrosion inhibition. The present study aims to comprehensively investigate the corrosion inhibition performance of TET through a combination of experimental techniques and theoretical approaches. Weight loss assessment, a widely employed method for corrosion evaluation, serves as the primary experimental technique, allowing for the determination of inhibition efficiency under varying conditions. The immersion time and temperature are crucial parameters influencing the corrosion process, and their impact on TET's inhibitive properties will be systematically examined. In addition to the experimental investigations, the study employs Density Functional Theory (DFT) to gain insights into the molecular-level interactions between TET and the mild steel alloy surface.

DFT has proven to be a powerful tool in elucidating the electronic structure, reactivity, and adsorption characteristics of molecules on metal surfaces. Theoretical studies, including the Highest Occupied Molecular Orbital (E_{HOMO}) and Lowest Unoccupied Molecular Orbital (E_{LUMO}), will be conducted to understand the electronic properties of TET and its potential for adsorption on the metal surface [23–31]. The investigation of corrosion inhibition mechanisms is essential for developing a profound understanding of how TET interacts with the mild steel alloy at the molecular level. This understanding is crucial for the rational design of more effective corrosion inhibitors. Additionally, the study aims to correlate the experimental findings with theoretical insights, bridging the gap between macroscopic observations and molecular-level understanding. The overarching objective of this research is to contribute valuable knowledge to the field of corrosion science and materials protection. By elucidating the corrosion inhibition performance of TET (Figure 1), we aim to provide insights that can inform the design and development of novel and efficient corrosion inhibitors. The findings of this study could potentially have practical implications in industries where mild steel alloys are exposed to corrosive environments, offering a sustainable approach to enhance the durability and lifespan of metallic materials. The novelty of this work lies in its dual approach to investigating corrosion inhibition. By combining traditional weight loss experiments with advanced quantum chemical calculations, the study offers a comprehensive understanding of the effectiveness of Schiff base derivatives as corrosion inhibitors for mild steel in acidic environments. This

multidisciplinary approach provides novel insights into the mechanisms underlying corrosion inhibition and offers valuable contributions to the development of more effective and environmentally friendly corrosion protection strategies.

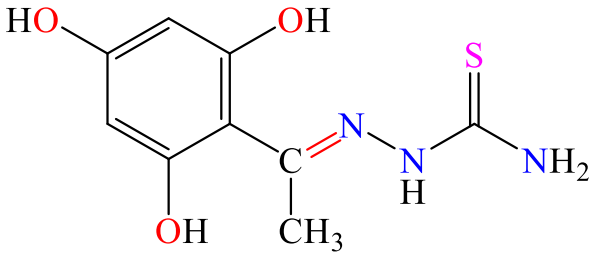

Figure 1. The molecular structure of TET.

2. Experimental part

2.1. Composition of material samples

The mild steel coupons employed in this study were rectangular in shape, measuring 2.0×2.5×0.1 cm. The material composition, determined as 0.21 wt.% carbon, 0.09 wt.% phosphorus, 0.05 wt.% manganese, 0.038 wt.% silicon, 0.01 wt.% aluminum, 0.050 wt.% sulfur, and iron (balance), reflects the typical composition of mild steel. Prior to experimentation, the specimen surfaces underwent meticulous mechanical polishing using various emery papers. Subsequently, the samples were cleansed with double-distilled water, degreased with acetone, and subjected to drying within a desiccator. The hydrochloric acid solution (1 M) utilized in the experiments was freshly prepared by diluting 37% analytical grade hydrochloric acid with distilled water.

2.2. Weight loss measurements

The weight loss measurements were carried out in a non-stirred, aerated hydrochloric acid solution freshly prepared at a concentration of 1 M. Gravimetric techniques were employed by assessing the weight difference in the absence and presence of TET as a corrosion inhibitor in the corrosive environment. Various concentrations of TET (0.1, 0.2, 0.3, 0.4, 0.5, and 1.0 mM) served as electrolytes for the gravimetric experiments [32, 33]. The immersion periods of 1, 2, 5, 10, and 24 hours were chosen for weight loss measurements. Throughout the experiments, the temperature of each electrolyte was rigorously maintained using a thermostatically regulated water bath. Coupons were immersed in the electrolytes at temperatures of 303, 313, 323, and 333 K for a standardized duration of five hours. The experiments were conducted in triplicate to ensure precision, and the average values of weight loss were computed to enhance reproducibility. The corrosion rate (C_R), surface coverage (θ), and inhibition efficiency (*IE*) were determined from the gravimetric data in accordance with ASTM standards, employing Equations 1–3 [34–36].

$$C_{\mathrm{R}} = \frac{87.6W}{d \cdot a \cdot t} \tag{1}$$

W is the weight loss, d is the density, a is the surface area and t is the immersion time.

$$IE\% = \frac{C_{\mathrm{R}_0} - C_{\mathrm{R}}}{C_{\mathrm{R}_0}} \cdot 100 \tag{2}$$

$$\theta = \frac{C_{\mathrm{R}_0} - C_{\mathrm{R}}}{C_{\mathrm{R}_0}} \tag{3}$$

2.3. Computational study

The electronic structure of the TET molecule was investigated through a computational quantum chemical modeling technique employing density functional theory (DFT). The DFT calculations were performed using the B3LYP functional with a 6-31G basis set, facilitating the determination of the TET molecule's geometry optimization. The highest occupied molecular orbital (HOMO) and lowest unoccupied molecular orbital (LUMO) were identified as the frontier molecular orbitals. These orbitals were utilized to estimate crucial parameters, including the energy gap (ΔE), global hardness (η), softness (σ), absolute electronegativity (χ), and the number of transferred electrons (ΔN), as per Equations 4–8 [37, 39].

$$\Delta E = E_{\mathrm{HOMO}} - E_{\mathrm{LUMO}} \tag{4}$$

$$\eta = -\frac{E_{\mathrm{HOMO}} - E_{\mathrm{LUMO}}}{2} \tag{5}$$

$$\sigma = \frac{1}{\eta} \tag{6}$$

$$\chi = -\frac{E_{\mathrm{HOMO}} + E_{\mathrm{LUMO}}}{2} \tag{7}$$

$$\Delta N = \frac{7 - \chi}{2(\eta)} \tag{8}$$

3. Results and Discussion

3.1. Weight loss measurements

The corrosion rate (C_{R}) of mild steel in 1 M HCl was evaluated through weight loss measurements at temperatures of 303, 313, 323, and 333 K in the presence of TET. Figure 2 illustrates the quantitative data, revealing a noteworthy increase in inhibition efficiency with increasing TET concentration at 303 K. At a 0 mM inhibitor concentration, the mild steel C_{R}

was 4.31 ($mg \cdot cm^{-2} \cdot h^{-1}$). However, at the optimal TET concentration of 0.39 C_R ($mg \cdot cm^{-2} \cdot h^{-1}$), a substantial decrease in corrosion rate was observed at 303 K. This concentration-dependent decrease in weight loss underscores the inhibitory effect of TET on mild steel corrosion in hydrochloric acid. The experimental findings demonstrate that TET hinders corrosion, lowers the corrosion rate, and enhances inhibition efficiency as the inhibitor concentration increases [40–44]. Remarkably, TET exhibited remarkable inhibition efficiency, reaching 90.2% at a concentration of 0.05 mM over a five-hour exposure period. The nitrogen and sulfur heteroatoms in TET contribute to its inhibitive behavior, fostering a reactive interaction with the mild steel surface. The resonance effect and molecular stability further enhance TET's inhibition efficiency.

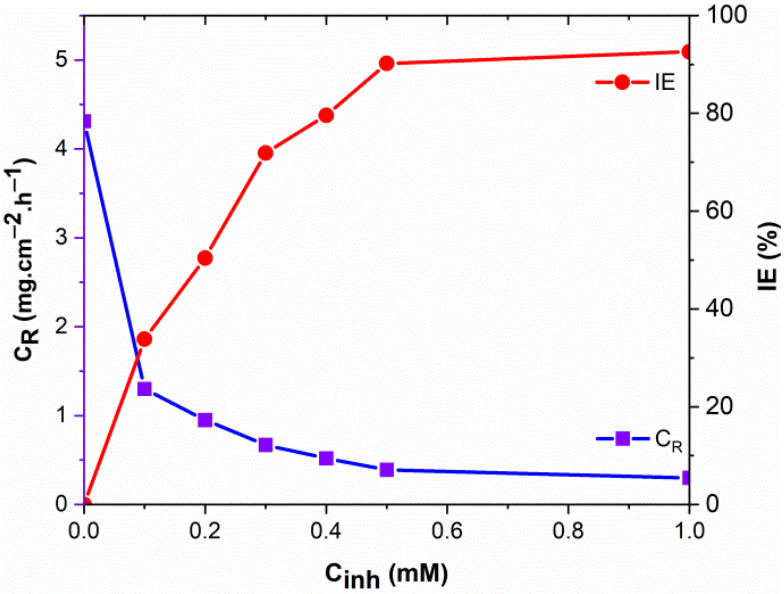

Figure 2. Variation of C_R and *IE*% with different concentration of TET for 5 hours as immersion time at 303 K for mild steel in 1 M HCl.

3.2. Effect of immersion time

Time-dependent investigations on the impact of corrosion inhibitors are crucial for understanding their efficacy over varying exposure durations. The stability of the protective film formed by TET and its adsorption rate were systematically explored across different immersion times (1, 5, 10, 24 and 48 hours) [45–47]. The results revealed notable trends in the corrosion rate and inhibition efficiency, shedding light on the dynamic nature of TET's protective effects. The data showcases a compelling relationship between immersion time, corrosion rate, and inhibition efficiency. Based on Figure 3, the corrosion rate decreases with increasing immersion time up to a certain point, emphasizing the effectiveness of TET in mitigating corrosion over short to moderate exposure durations. For instance, at a concentration of 0.1 mM, the corrosion rate decreases from 1.39 $mg \cdot cm^{-2} \cdot h^{-1}$ at 1 hour to 0.9 $mg \cdot cm^{-2} \cdot h^{-1}$ at 10 hours, highlighting a substantial reduction in corrosion with prolonged exposure [48, 49]. However, a nuanced trend emerges as the immersion time

extends to 24 hours. Inhibition efficiency tends to decrease at longer immersion periods, indicating a diminishing protective effect. This decline is attributed to the desorption of TET molecules from the coupon surface, suggesting a temporary nature of the inhibitor's film [50, 51]. In summary, the numerical results underscore the time-sensitive nature of TET's corrosion inhibition mechanism. While the inhibitor exhibits strong protective effects over short to moderate immersion times, the diminishing inhibition efficiency at longer exposures emphasizes the need for careful consideration of immersion durations in practical applications. These findings provide valuable insights for optimizing the deployment of TET as a corrosion inhibitor under various exposure conditions.

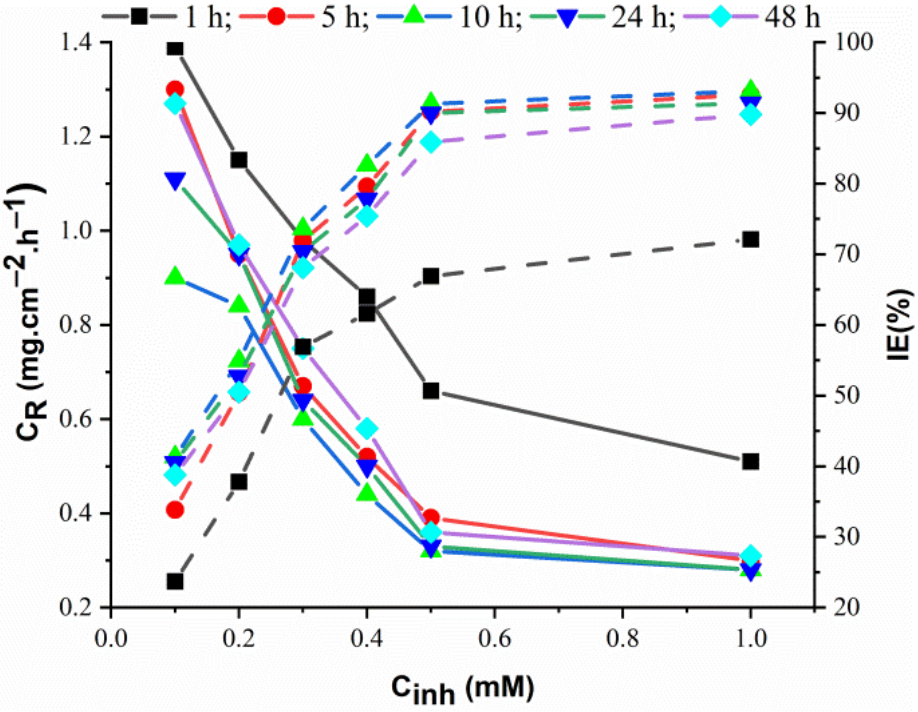

Figure 3. Variation of C_R and *IE*% with different concentration of TET for various immersion time at 303 K for mild steel in 1 M HCl.

3.3. Effect of temperature

The impact of temperature on both the corrosion rate and the inhibitive activity of TET was systematically explored. The addition of TET led to unimportant reduction in the corrosion rate, attributed to potential interactions between TET molecules and the coupon surface. This interaction facilitated the formation of a protective layer, with TET molecules adsorbed onto the coupon surface, effectively shielding it from the corrosive hydrochloric acid solution. The weight loss measurements provided insights into the variation in corrosion rate at different solution temperatures, namely 303, 313, 323, and 333 K [52, 53]. The relationship between the corrosion rate and temperature is graphically represented in Figure 4, utilizing an Arrhenius plot calculated according to Equation 9 [54, 55]:

$$C_R = A\exp\left(-\frac{E_a}{RT}\right) \quad (9)$$

Here, A represents the pre-exponential factor, E_a is the activation energy, R is the gas constant, and T is the absolute temperature.

The activation energy value in the presence of TET suggests that the inhibitor molecules were adsorbed onto the coupon surface through a chemisorption mechanism. The results of weight loss calculations are presented in Figure 5, illustrating the decrease in inhibition efficiency (*IE*%) with rising temperatures. In the present study, TET demonstrated a substantial inhibition efficiency of 90.2% at 303 K, but this efficiency decreased to 76.4% at 333 K. The observed trend indicates an exothermic mechanism at higher temperatures in the tested solution [56, 57]. The temperature-dependent performance of TET reveals a nuanced relationship between temperature and inhibition efficiency. While TET exhibits excellent inhibition efficiency in hydrochloric acid at room temperature, its inhibitive performance diminishes at higher temperatures, as evidenced by the decline shown in Figure 5 [58, 59]. This temperature sensitivity suggests that the inhibitive mechanism of TET is influenced by the energy changes associated with the corrosion process, emphasizing the need for a thorough understanding of temperature effects in designing effective corrosion inhibitors for varying environmental conditions [60]. The detailed examination of the effect of temperature on TET's inhibition efficiency provides valuable insights for optimizing its application in real-world corrosion prevention scenarios [61, 62].

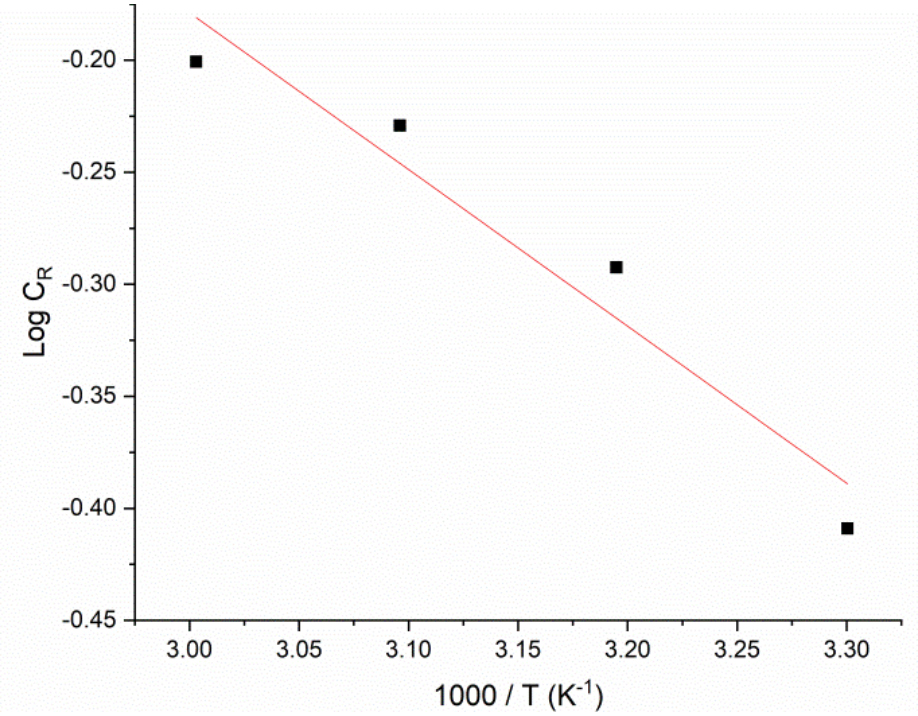

Figure 4. The Arrhenius plot for mild steel corrosion in acidic solution in the presence of TET (0.5 mM) at various temperatures.

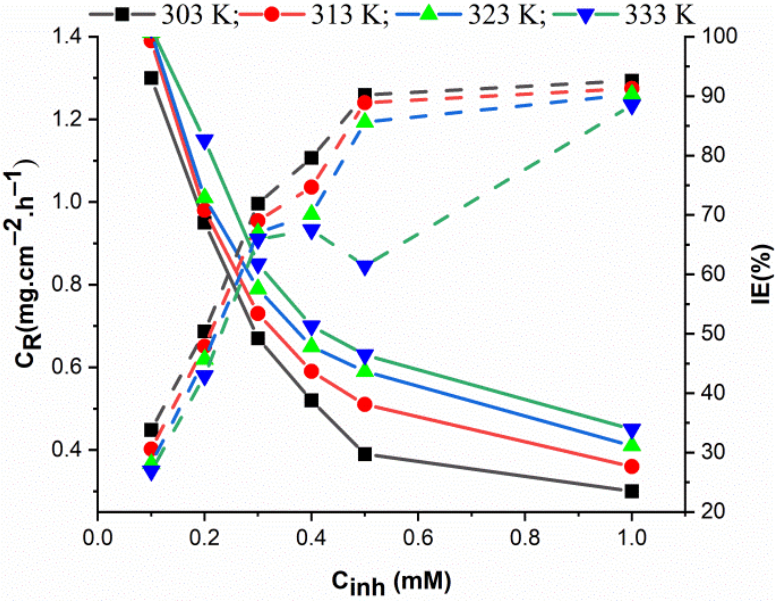

Figure 5. Variation of C_R and *IE*% with a different concentration of TET for various temperature in 1 M HCl.

3.4. Adsorption isotherms

In the realm of acid corrosion, the prevailing understanding is that inhibitor molecules exert their influence on metal surfaces through an adsorption mechanism. This adsorption process is believed to alter the structural charge of the double layer, reducing the rate of partial electrochemical reactions. Primarily occurring at active sites on the metal surface, adsorption impedes the reactivity of the metal during the dissolution process [63–65]. Additionally, if the reduction of inhibitor molecules aligns with adsorption, a solid film may form, acting as a protective barrier. Understanding the adsorption behavior of inhibitor molecules is crucial for elucidating their mechanism of action. Adsorption isotherms provide insight into the relationship between the coverage of adsorbate molecules at the interface and the concentration of the solution's material [66–68]. Surface coverage (θ) for TET was obtained using the weight loss technique, and it was instrumental in evaluating the adsorption isotherm model. Investigating adsorption isotherms is imperative for comprehending the intricacies of interactions between inhibitor molecules and the mild steel surface, where adsorption can occur through either physical or chemical reactions. Different isotherms, such as Langmuir, Temkin, and Freundlich, can be employed to interpret the phenomenon of adsorption [69–72]. Fitting the data into established adsorption isotherms, as depicted in Figure 6, enables an understanding of the adsorbent nature of the inhibitor's performance. Notably, the adsorption of TET molecules on the mild steel surface aligns with the Langmuir isothermal adsorption model, supported by a high regression coefficient value (R^2=0.968). The Langmuir model plot, illustrating the relationship between C/θ and C, is indicative of the adsorption process's linearity. The Langmuir model's slope and intercept values are 1.42 and 0.225, respectively. The evaluation of K_{ads} by Equation 10 allows for further insights into the adsorption process [73–77]. Moreover, the determination of free energy (G_{ads})

through Equation 11 provides a critical parameter for understanding the nature of the interaction between TET molecules and the coupon surface [78–80].

$$\frac{C_{\text{inh}}}{\theta} = \frac{1}{K_{\text{ads}}} + C_{\text{inh}} \tag{10}$$

$$\Delta G^{0}_{\text{ads}} = -RT \ln\left(55.5 K_{\text{ads}}\right) \tag{11}$$

Where 55.5 is water concentration, R is gaseous constant, and T is the absolute temperature.

The calculated G_{ads} value for TET is 31.85 kJ·mol^{-1}. According to established literature [13, 47], $\Delta G^{0}_{\text{ads}}$ values below –20 kJ·mol^{-1} suggest physical adsorption, while values above –40 kJ·mol^{-1} indicate chemical adsorption [81–83]. With a G_{ads} value of –31.85 kJ·mol^{-1}, the interaction nature between TET molecules and the tested coupon surface is classified as chemisorption. This underscores that, while the initial adsorption process may involve physical adsorption, the dominant model for adsorption, as suggested by the G_{ads} value, is chemical adsorption [84–87]. This detailed insight into the adsorption isotherms of TET on mild steel surfaces enhances our understanding of its corrosion inhibition mechanism.

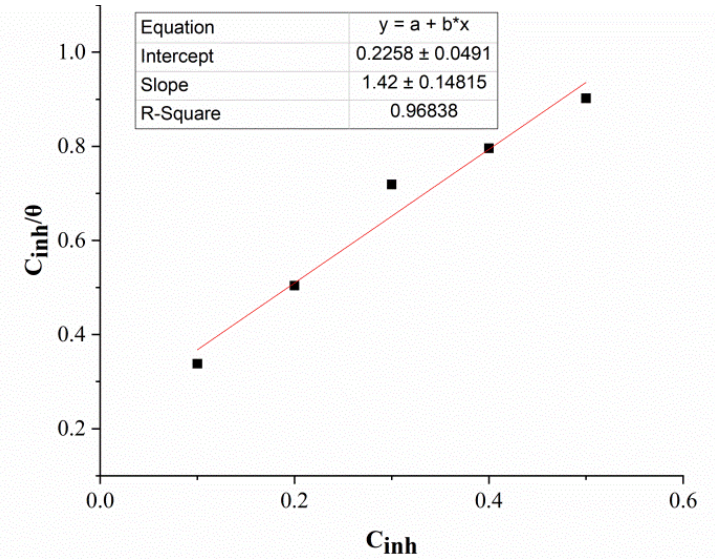

Figure 6. Langmuir adsorption model of TET.

3.5. Density Functional Theory analysis

The exploration of Density Functional Theory (DFT) parameters offers quantitative insights into the inhibitive performance and the underlying inhibition mechanism of the TET molecule. Quantum chemical factors, including frontier Molecular Orbitals (HOMO and LUMO), energy gap (ΔE), electronegativity (χ), global hardness (η), softness (σ), a fraction of transferred electrons (ΔN), and atomic charges, serve as critical indicators in deciphering molecular interactions and stability [88]. The optimized molecular structure of TET, illustrated in Figure 7, reflects the outcome of DFT studies. The HOMO value of –6.93 eV

denotes the molecule's ability to donate electrons to the vacant d-orbitals of iron, while the LUMO value of –0.104 eV indicates its capacity to accept electrons from iron. The relatively high HOMO value suggests efficient electron donation, aligning well with the experimental findings [89]. Conversely, the low LUMO value suggests that the inhibitor molecule can effectively accept electrons from iron through a backdonation mechanism. The energy gap (ΔE) is a crucial parameter, and its numerical value of 6.826 eV in TET indicates a substantial inhibition efficiency. The global hardness (η) and softness (σ) values provide additional quantitative information on molecular stability and reactivity. A high energy gap, coupled with low softness (0.293 eV^{-1}) and high global hardness (3.413 eV), points to significant inhibitive efficiency. TET's complex molecular structure, characterized by a high energy gap, aligns with the observed inhibitive performance [90].

Density Functional Theory analysis suggests that molecules with a high value of softness and low global hardness exhibit significant inhibitive efficiency. The obtained σ value of 0.293 eV^{-1} implies that TET readily adsorbs on the coupon surface, further supporting its experimental inhibitory effectiveness. The high negative atomic charges, particularly in nitrogen and sulfur atoms (ΔN=0.509), enhance the molecule's ability to be adsorbed on the coupon surface, forming strong coordination bonds with the mild steel [91]. The correlation between experimental findings, numerical quantum parameters, and atomic charges strengthens the understanding of TET's inhibition mechanism. The coordinated adsorption of TET on the mild steel surface, as suggested by its high inhibitive efficiency (90.2%), is supported by the quantifiable DFT-derived molecular properties. This integrated approach, combining numerical and experimental insights, not only enhances our comprehension of TET's corrosion inhibition potential but also provides a quantitative foundation for designing and optimizing effective corrosion inhibitors.

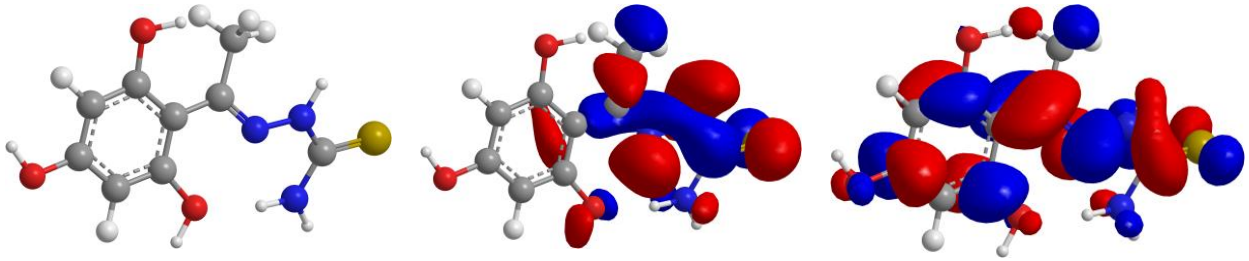

Figure 7. Optimized structure, Highest Occupied MO, and Lowest Unoccupied MO of TET molecules.

3.6. Atomic charges

The atomic charges assigned to each atom in the TET molecule provide crucial insights into its chemical reactivity and its potential for interaction with the mild steel surface. The numerical values of these atomic charges (Figure 8), calculated through Density Functional

Theory (DFT), offer a quantitative representation of electron distribution within the molecule [92].

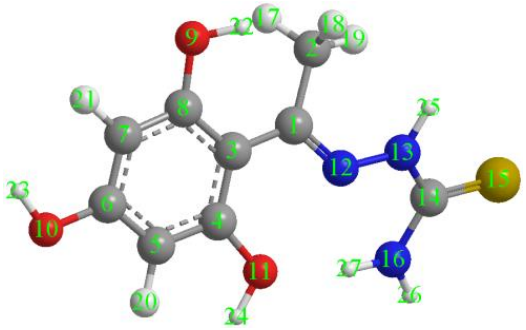

Figure 8. Optimized structure with atomic numbers.

The atomic charges such as carbon atoms (C(1): 0.0584126; C(2): −0.185304; C(3): −0.130625; C(4): 0.23369; C(5): −0.22252; C(6): 0.23284; C(7): −0.225393; C(8): 0.234952). The varying charges on carbon atoms indicate their different roles within the molecule. For instance, C(1) and C(4) have positive charges, suggesting electron-donating capabilities, while C(2), C(3), C(5), C(7), and C(16) exhibit negative charges, indicating their ability to accept electrons. The negative charges on oxygen atoms (O(9) −0.311963; O(10) −0.266456; O(11) −0.26044) signify their electron-accepting nature. These oxygen atoms may play a crucial role in forming coordination bonds with metal surfaces. Nitrogen atoms (N(12) −0.177065; N(13) 0.319529; N(16) −0.0370558) exhibit a range of charges. N(13) carries a positive charge, indicating its potential to donate electrons, while N(12) and N(16) have negative charges, suggesting their affinity for accepting electrons. The significant negative charge on the sulfur atom (S(15) −0.652052) suggests a strong capability to accept electrons, emphasizing its potential involvement in the adsorption process on the metal surface. The distribution of atomic charges provides valuable information on the polarity and reactivity of different atoms within the TET molecule. These charges play a pivotal role in dictating the molecule's interaction with the mild steel surface. Specifically, atoms with higher negative charges, such as oxygen, nitrogen, and sulfur, are likely to form coordination bonds with metal surfaces, contributing to the observed inhibitive efficiency of TET in the experimental corrosion inhibition study.

Density Functional Theory (DFT) calculations were performed to investigate the electronic structure and properties of the 1-(2,4,6-trihydroxyphenyl)ethanone thiosemicarbazone (TET) molecule. The computed DFT parameters, including the Highest Occupied Molecular Orbital (HOMO), Lowest Unoccupied Molecular Orbital (LUMO), energy gap (ΔE), global hardness (η), softness (σ), and the fraction of transferred electrons (ΔN), offer valuable insights into TET's inhibitory behavior. To contextualize these DFT results, comparison with similar values for other corrosion inhibitors is essential to understand their correlation with protective effects. Previous studies have reported DFT calculations for various organic compounds used as corrosion inhibitors, highlighting the

relationship between molecular properties and inhibitory performance. By comparing the computed DFT parameters of TET with those of other inhibitors, we can assess their relative effectiveness and gain insights into the underlying inhibitory mechanisms. For example, studies have shown that inhibitors with lower energy gaps (ΔE) and higher softness (σ) values tend to exhibit enhanced inhibitory efficiency due to their greater reactivity and adsorption affinity towards metal surfaces. Furthermore, the fraction of transferred electrons (ΔN) provides information about the electron-donating or accepting capabilities of the inhibitor molecules, which play a crucial role in their interaction with metal ions and corrosion products. By analyzing the DFT results in conjunction with experimental data on protective effects, we can establish correlations between molecular properties and inhibitory performance, thereby elucidating the mechanisms governing corrosion inhibition. Future research endeavors will focus on expanding this comparative analysis to encompass a broader range of inhibitors and experimental conditions, further enhancing our understanding of corrosion inhibition mechanisms and facilitating the development of more effective inhibitors [93–95].

3.7. Suggested inhibition mechanism

The inhibitive performance of TET in hydrochloric acid solution is likely governed by a complex yet well-defined inhibition mechanism. The synergy between experimental findings and quantum chemical insights aids in proposing a plausible inhibition mechanism that elucidates the protective role of TET on mild steel surfaces [95, 96].

1. Adsorption process: The molecular adsorption of TET on the mild steel surface is a fundamental step in its inhibition mechanism. The quantum chemical parameters, including HOMO, LUMO, and atomic charges, emphasize the molecule's propensity to interact with metal surfaces. Notably, the significant negative charges on nitrogen and sulfur atoms enhance the adsorption potential of TET. The adsorption process involves the formation of coordination bonds between TET and the metal surface, creating a protective layer that shields the metal from corrosive attacks.
2. Donation and acceptance of electrons: The HOMO-LUMO analysis provides insights into the electron-donating and accepting capabilities of TET. The relatively high HOMO value indicates the molecule's ability to donate electrons to the vacant d-orbitals of iron, facilitating the formation of stable coordination bonds. Conversely, the low LUMO value suggests the molecule's capacity to accept electrons from iron, further reinforcing its role in the inhibition mechanism through backdonation.
3. Atomic charges and coordination bonds: The atomic charges assigned to each atom in TET play a crucial role in understanding the inhibition mechanism. Oxygen, nitrogen, and sulfur atoms, possessing significant negative charges, are more likely to engage in coordination bonds with metal atoms on the surface. These bonds contribute to the formation of a protective layer, impeding the corrosion process.

4. Formation of protective barrier: The adsorption of TET molecules on the mild steel surface forms a protective barrier, hindering the access of corrosive agents to the metal surface. The Langmuir adsorption isotherm model, supported by the calculated adsorption parameters, reinforces the formation of a stable adsorbed layer, explaining the observed inhibition efficiency.
5. Time and temperature dependence: The inhibition mechanism is also influenced by the immersion time and temperature. The highest inhibition activity observed at 5 hours may be attributed to the rapid adsorption of TET molecules, forming a protective layer on the metal surface. However, at longer immersion times, desorption becomes more prominent, leading to a decrease in inhibition efficiency. The temperature dependence indicates that the inhibitive performance is favorable at lower temperatures, suggesting an exothermic mechanism.

In summary, the suggested inhibition mechanism involves the adsorption of TET molecules on the mild steel surface, facilitated by coordination bonds formed through the donation and acceptance of electrons. The resulting protective layer acts as a barrier, impeding the corrosion process. The proposed mechanism aligns with both experimental observations and quantum chemical insights, providing a comprehensive understanding of TET's corrosion inhibition potential.

3.8. Comparison with similar research works

The inhibitory mechanism of 1-(2,4,6-trihydroxyphenyl)ethanone thiosemicarbazone (TET) against mild steel corrosion in acidic environments was investigated using weight loss techniques and Density Functional Theory (DFT) analysis. Existing literature underscores the effectiveness of corrosion inhibitors, particularly those containing nitrogen, oxygen, sulfur, π-bonds, and resonance effects, in combating HCl-induced corrosion of mild steel. It is widely acknowledged that inhibitors possessing a combination of these elements exhibit superior inhibitory performance compared to those with only one of them. The prevailing assumption is that the adsorption mechanism primarily involves the nitrogen, sulfur, and oxygen atoms within the organic molecules. Numerous scholarly works emphasize the significance of organic corrosion inhibitors featuring electron donor atoms such as phosphorus, sulfur, oxygen, and nitrogen for surface adsorption on metals, thereby safeguarding against acidic solutions. Among these heteroatoms, nitrogen demonstrates notable inhibitive efficacy, followed by phosphorus, sulfur, and oxygen. Natural plant extracts have garnered attention for their commendable attributes, including cost-effectiveness, renewability, biodegradability, and environmental friendliness. However, organic inhibitors may encounter challenges related to limited solubility in polar electrolytes due to their inherent hydrophobic nature. Typically, organic corrosion inhibitors comprise nitrogen, hydrophobic hydrocarbon chains, sulfur, and oxygen moieties in their molecular structures. The effectiveness of these inhibitors hinges on various factors such as molecular size, aromaticity, bonding atoms or groups (π or σ), charge distribution, and electronic

structure. Computational chemistry techniques like DFT have proven invaluable in elucidating the inhibitory properties of organic compounds. The inhibitory efficiency of TET was compared with other nitrogen-containing corrosion inhibitors for safeguarding mild steel against corrosion. For instance, a corrosion inhibitor, namely 7-((1-(4-fluorobenzyl)-1*H*-1,2,3-triazol-4-yl)methyl)-1,3-dimethyl-3,7-dihydro-1*H*-purine-2,6-dione, exhibited an inhibition efficiency of 86%. However, this compound exhibited lower efficiency compared to TET. Similarly, corrosion inhibitors like 3,5-di(*m*-tolyl)-4-amino-1,2,4-triazole, 3-salicylialidene amino-1,2,4-triazole phosphonate, 3-benzylidene amino-1,2,4-triazole phosphonate, 3-*p*-nitro-benzylidene amino-1,2,4-triazole phosphonate, and 1-amino-3-methyl thio-1,2,4-triazole, despite containing a triazole ring and amino group, exhibited much lower inhibition efficiencies (24%, 63%, 56%, 69%, and 43%, respectively) compared to the studied inhibitor. Another study investigated the use of 3,5-Bis(methylene octadecyldimethylammonium chloride)-1,2,4-triazole as a corrosion inhibitor. Although it demonstrated high inhibition efficiency (98%), its high cost rendered it less favorable. In contrast, TET, while easy to synthesize and stable, exhibited an inhibition efficiency of 90%, slightly lower than that of the studied inhibitor [97–100]. TET displayed superior inhibitory efficiency compared to the aforementioned compounds and exhibited efficiency levels comparable to those described in previous studies. Moreover, as the concentration of TET increased, the corrosion rate decreased, indicating an enhancement in inhibitive efficacy, possibly attributable to increased adsorption of the inhibitor on the mild steel surface with increasing concentration.

4. Conclusion

Our study explored how well a new compound (TET) can prevent mild steel from rusting in acidic water (hydrochloric acid). We used various methods to understand how TET works and how effective it is. The results showed that TET is very effective in preventing rust, reaching almost 90% protection under ideal conditions. Adding more TET increased this protection, but it worked slightly better at cooler temperatures. Further analysis suggests TET forms a protective layer on the steel surface. We used computer modeling to examine the molecule's structure and properties to understand this process better. This analysis helped explain how TET interacts with the metal to prevent corrosion. Overall, this research shows that TET has great potential as a rust preventative. It paves the way for designing even more effective and environmentally friendly solutions to protect metals from rust, especially in acidic environment

References

1. M. Lagrenée, B. Mernari, M. Bouanis, M. Traisnel and F. Bentiss, Study of the mechanism and inhibiting efficiency of 3,5-bis(4-methylthiophenyl)-4*H*-1,2,4-triazole on mild steel corrosion in acidic media, *Corros. Sci*., 2002, **44**, no. 3, 573–588. doi: 10.1016/S0010-938X(01)00075-0

2. Y.G. Avdeev, Protection of metals in phosphoric acid solutions by corrosion inhibitors. Review, *Int. J. Corros. Scale Inhib*., 2019, **8**, no. 4, 760–798. doi: 10.17675/2305-6894-2019-8-4-1
3. H.H. Hassan, E. Abdelghani and M.A. Amin, Inhibition of mild steel corrosion in hydrochloric acid solution by triazole derivatives. Part I. Polarization and EIS studies, *Electrochim. Acta*, 2007, **52**, no. 22, 6359–6366. doi: 10.1016/j.electacta.2007.04.046
4. M.M. Solomon, I.E. Uzoma, J.A.O. Olugbuyiro and O.T. Ademosun, A Censorious Appraisal of the Oil Well Acidizing Corrosion Inhibitors, *J. Pet. Sci. Eng*., 2022, **215**, 110711. doi: 10.1016/j.petrol.2022.110711
5. E. Abdullayev, R. Price, D. Shchukin and Y. Lvov, Halloysite tubes as nanocontainers for anticorrosion coating with benzotriazole, *ACS Appl. Mater. Interfaces*, 2009, **1**, no. 7, 1437–1443. doi: 10.1021/am9002028
6. K.R. Ansari, M.A. Quraishi and A. Singh, Schiff's base of pyridyl substituted triazoles as new and effective corrosion inhibitors for mild steel in hydrochloric acid solution, *Corros. Sci*., 2014, **79**, 5–15. doi: 10.1016/J.CORSCI.2013.10.009
7. A.D. Becke, Density-functional exchange-energy approximation with correct asymptotic behavior, *Phys. Rev. A*, 1988, **38**, no. 6, 3098. doi: 10.1103/PhysRevA.38.3098
8. C. Lee, W. Yang and R.G. Parr, Development of the Colle-Salvetti correlation-energy formula into a functional of the electron density, *Phys. Rev. B*, 1988, **37**, no. 2, 785. doi: 10.1103/PhysRevB.37.785
9. W.P. Singh and J. Bockris, Toxicity issues of organic corrosion inhibitors: applications of QSAR model, *Corrosion*, **96**, 1996.
10. K. Khaled, Modeling corrosion inhibition of iron in acid medium by genetic function approximation method: A QSAR model, *Corros. Sci*., 2011, **53**, no. 11, 3457–3465. doi: 10.1016/j.corsci.2011.01.035
11. M. Shabani-Nooshabadi, M. Behpour, F.S. Razavi, M. Hamadanian and V. Nejadshafiee, Study of *N*-benzylidene derivatives synthesized as corrosion inhibitors for copper in HCl solution, *RSC Adv*., 2015, **5**, no. 30, 23357–23366. doi: 10.1039/C5RA00561B
12. H. Gilson, B.H. Honig, A. Croteau, G. Zarrilli and K. Nakanishi, Analysis of the factors that influence the C=N stretching frequency of polyene Schiff bases. Implications for bacteriorhodopsin and rhodopsin, *Biophys. J*., 1988, **53**, no. 2, 261–269. doi: 10.1016/S0006-3495(88)83087-X
13. T. Baasov, N. Friedman and M. Sheves, Factors affecting the C:N stretching in protonated retinal Schiff base: a model study for bacteriorhodopsin and visual pigments, *Biochemistry*, 1987, **26**, no. 11, 3210–3217. doi: 10.1021/bi00385a041
14. H.P. Ebrahimi, J.S. Hadi, Z.A. Abdulnabi and Z. Bolandnazar, Spectroscopic, thermal analysis and DFT computational studies of salen-type Schiff base complexes, *Spectrochim. Acta, Part A*, 2014, **117**, 485–492. doi: 10.1016/j.saa.2013.08.044

15. J. Ortega-Castro, M. Adrover, J. Frau, A. Salvà, J. Donoso and F. Muñoz, DFT studies on Schiff base formation of vitamin B6 analogues. Reaction between a pyridoxamine-analogue and carbonyl compounds, *J. Phys. Chem. A*, 2010, **114**, no. 13, 4634–4640. doi: 10.1021/jp909156m
16. A.N. Jasim, B.A. Abdulhussein, S. Mohammed Noori Ahmed, W.K. Al-Azzawi, M.M. Hanoon, M.K. Abbass and A.A. Al-Amiery, Schiff's base performance in preventing corrosion on mild steel in acidic conditions, *Prog. Color, Color. Coat.*, 2023, **16**, no. 4, 319–329. doi: 10.30509/PCCC.2023.167081.1197
17. B.S. Mahdi, M.K. Abbass, M.K. Mohsin, W.K. Al-Azzawi, M.M. Hanoon, M.H.H. AlKaabi, L.M. Shaker, A.A. Al-Amiery, W.N.R.W. Isahak, A.A.H. Kadhum and M.S. Takriff, Corrosion inhibition of mild steel in hydrochloric acid environment using terephthaldehyde based on Schiff base: Gravimetric, thermodynamic, and computational studies, *Molecules*, 2022, **27**, no. 15, 4857. doi: 10.3390/molecules27154857
18. D.S. Chauhan, M.A.J. Mazumder, M.A. Quraishi and K.R. Ansari, Chitosan-Cinnamaldehyde Schiff Base: A Bioinspired Macromolecule as Corrosion Inhibitor for Oil and Gas Industry, *Int. J. Biol. Macromol.*, 2020, **158**, 127–138. doi: 10.1016/j.ijbiomac.2020.04.200
19. S. Şafak, B. Duran, A. Yurt and G. Türkoğlu, Schiff Bases as Corrosion Inhibitor for Aluminium in HCl Solution, *Corros. Sci.*, 2012, **54**, 251–259. doi: 10.1016/j.corsci.2011.09.026
20. A. Alamiery, L.M. Shaker, T. Allami, A.H. Kadhum and M.S. Takriff, A study of acidic corrosion behavior of Furan-Derived Schiff base for mild steel in hydrochloric acid environment: Experimental, and surface investigation, *Mater. Today: Proc.*, 2021, **44**, 2337–2341. doi: 10.1016/j.matpr.2020.12.431
21. A. Alamiery, E. Mahmoudi and T. Allami, Corrosion inhibition of low-carbon steel in hydrochloric acid environment using a Schiff base derived from pyrrole: gravimetric and computational studies, *Int. J. Corros. Scale Inhib.*, 2021, **10**, no. 2, 749–765. doi: 10.17675/2305-6894-2021-10-2-17
22. A.M. Resen, M. Hanoon, R.D. Salim, A.A. Al-Amiery, L.M. Shaker and A.A.H. Kadhum, Gravimetrical, theoretical, and surface morphological investigations of corrosion inhibition effect of 4-(benzoimidazole-2-yl) pyridine on mild steel in hydrochloric acid, *Koroze Ochr. Mater.*, 2020, **64**, no. 4, 122–130. doi: 10.2478/kom-2020-0018
23. W.K. Al-Azzawi, S.M. Salih, A.F. Hamood, R.K. Al-Azzawi, M.H. Kzar, H.N. Jawoosh, L.M. Shakier, A. Al-Amiery, A.A.H. Kadhum, W.N.R.W. Isahak and M.S. Takriff, Adsorption and theoretical investigations of a Schiff base for corrosion inhibition of mild steel in an acidic environment, *Int. J. Corros. Scale Inhib.*, 2022, **11**, no. 3, 1063–1082. doi: 10.17675/2305-6894-2022-11-3-10
24. H.S. Aljibori, A.H. Alwazir, S. Abdulhadi, W.K. Al-Azzawi, A.A.H. Kadhum, L.M. Shaker, A.A. Al-Amiery and H.Sh. Majdi, The use of a Schiff base derivative to

inhibit mild steel corrosion in 1 M HCl solution: a comparison of practical and theoretical findings, *Int. J. Corros. Scale Inhib*., 2022, **11**, no. 4, 1435–1455. doi: 10.17675/2305-6894-2022-11-4-2

25. A.A. Al-Amiery, F.F. Sayyid, A.M. Mustafa, S.I. Ibrahim, M.K. Mohsin, M.M. Hanoon, M.H.H. Al-Kaabi, A.H. Kadhum and W.N.R.W. Isahak, Gravimetric Measurements and Theoretical Calculations of 4-Aminoantipyrine Derivatives as Corrosion Inhibitors for Mild Steel in Hydrochloric Acid Solution: Comparative Studies, *Corros. Sci. Technol*., 2023, **22**, no. 2, 73–89. doi: 10.14773/cst.2023.22.73
26. M.M. Hanoon, A.M. Resen, A.A. Al-Amiery, A.A.H. Kadhum and M.S. Takriff, Theoretical and Experimental Studies on the Corrosion Inhibition Potentials of 2-((6-Methyl-2-Ketoquinolin-3-yl)Methylene) Hydrazinecarbothioamide for Mild Steel in 1 M HCl, *Prog. Color, Color. Coat*., 2022, **15**, 21–33.
27. Y.M. Abdulsahib, A.J.M. Eltmimi, S.A. Alhabeeb, M.M. Hanoon, A.A. Al-Amiery, T. Allami and A.A.H. Kadhum, Experimental and theoretical investigations on the inhibition efficiency of *N*-(2,4-dihydroxytolueneylidene)-4-methylpyridin-2-amine for the corrosion of mild steel in hydrochloric acid, *Int. J. Corros. Scale Inhib*., 2021, **10**, no. 3, 885–899. doi: 10.17675/2305-6894-2021-10-3-3
28. A.K. Khudhair, A.M. Mustafa, M.M. Hanoon, A. Al-Amiery, L.M. Shaker, T. Gazz, A.B. Mohamad, A.H. Kadhum and M.S. Takriff, Experimental and Theoretical Investigation on the Corrosion Inhibitor Potential of N-MEH for Mild Steel in HCl, *Prog. Color, Color. Coat*., 2022, **15**, no. 2, 111–122. doi: 10.30509/PCCC.2021.166815.1111
29. S. Al-Baghdadi, A. Al-Amiery, T. Gaaz and A. Kadhum, Terephthalohydrazide and isophthalo-hydrazide as new corrosion inhibitors for mild steel in hydrochloric acid: Experimental and theoretical approaches, *Koroze Ochr. Mater*., 2021, **65**, no. 1, 12–22. doi: 10.2478/kom-2021-0002
30. A. Alamiery, Anticorrosion effect of thiosemicarbazide derivative on mild steel in 1 M hydrochloric acid and 0.5 M sulfuric Acid: Gravimetrical and theoretical studies, *Mater. Sci. Energy Technol*., 2021, **4**, 263–273. doi: 10.1016/j.mset.2021.07.004
31. A.A. Alamiery, W.N.R.W. Isahak and M.S. Takriff, Inhibition of mild steel corrosion by 4-benzyl-1-(4-oxo-4-phenylbutanoyl)thiosemicarbazide: Gravimetrical, adsorption and theoretical studies, *Lubricants*, 2021, **9**, no. 9, 93. doi: 10.3390/lubricants9090093
32. B.D.B. Tiu and R.C. Advincula, Polymeric Corrosion Inhibitors for the Oil and Gas Industry: Design Principles and Mechanism, *React. Funct. Polym*., 2015, **95**, 25–45. doi: 10.1016/j.reactfunctpolym.2015.08.006
33. Yu.I. Kuznetsov, N.N. Andreev and S.S. Vesely, Why we reject papers with calculations of inhibitor adsorption based on data on protective effects, *Int. J. Corros. Scale Inhib*., 2015, **4**, no. 2, 108–109.
34. I. Annon, A. Abbas, W. Al-Azzawi, M. Hanoon, A. Alamiery, W. Isahak and A. Kadhum, Corrosion inhibition of mild steel in hydrochloric acid environment using thiadiazole derivative: Weight loss, thermodynamics, adsorption and computational investigations, *S. Afr. J. Chem. Eng*., 2022, **41**, 244–252. doi: 10.1016/j.sajce.2022.06.011

35. ASTM International, *Standard Practice for Preparing, Cleaning, and Evaluating Corrosion Test*, 2011, 1–9.
36. NACE International, *Laboratory Corrosion Testing of Metals in Static Chemical Cleaning Solutions at Temperatures below 93°C (200°F)*, TM0193-2016-SG, 2000.
37. M.J. Frisch, G.W. Trucks, H.B. Schlegel, G.E. Scuseria, M.A. Robb, J.R. Cheeseman, J.A. Montgomery, Jr., T. Vreven, K.N. Kudin, J.C. Burant, J.M. Millam, S.S. Iyengar, J. Tomasi, V. Barone, B. Mennucci, M. Cossi, G. Scalmani, N. Rega, G.A. Petersson, H. Nakatsuji, M. Hada, M. Ehara, K. Toyota, R. Fukuda, J. Hasegawa, M. Ishida, T. Nakajima, Y. Honda, O. Kitao, H. Nakai, M. Klene, X. Li, J.E. Knox, H.P. Hratchian, J.B. Cross, V. Bakken, C. Adamo, J. Jaramillo, R. Gomperts, R.E. Stratmann, O. Yazyev, A.J. Austin, R. Cammi, C. Pomelli, J.W. Ochterski, P.Y. Ayala, K. Morokuma, G.A. Voth, P. Salvador, J.J. Dannenberg, V.G. Zakrzewski, S. Dapprich, A.D. Daniels, M.C. Strain, O. Farkas, D.K. Malick, A.D. Rabuck, K. Raghavachari, J.B. Foresman, J.V. Ortiz, Q. Cui, A.G. Baboul, S. Clifford, J. Cioslowski, B.B. Stefanov, G. Liu, A. Liashenko, P. Piskorz, I. Komaromi, R.L. Martin, D.J. Fox, T. Keith, M.A. Al-Laham, C.Y. Peng, A. Nanayakkara, M. Challacombe, P.M.W. Gill, B. Johnson, W. Chen, M.W. Wong, C. Gonzalez and J.A. Pople, *Gaussian 03, Revision B. 05*, Gaussian, Inc., Wallingford, CT, 2004.
38. T. Koopmans, Ordering of wave functions and eigen-energies to the individual electrons of an atom, *Physica*, 1934, **1**, no. 1–6, 104–113 (in German). doi: 10.1016/S0031-8914(34)90011-2
39. M. Chen, S. Lu, G. Yuan, S. Yang and X. Du, Synthesis and Antibacterial Activity of some Heterocyclic β-Enamino Ester Derivatives with 1,2,3-triazole, *Heterocycl. Commun*., 2000, **6**, no. 5, 421–426. doi: 10.1515/HC.2000.6.5.421
40. Y.A. Al-Soud, M.N. Al-Dweri and N.A. Al-Masoudi, Synthesis, antitumor and antiviral properties of some 1,2,4-triazole derivatives, *Il Farmaco*, 2005, **36**, no. 9. doi: 10.1002/chin.200509119
41. M. Ur-Rahman, Y. Mohammad, K.M. Fazili, K.A. Bhat and T. Ara, Synthesis and biological evaluation of novel 3-*O*-tethered triazoles of diosgenin as potent antiproliferative agents, *Steroids*, 2017, **118**, 1–8. doi: 10.1016/j.steroids.2016.11.003
42. M. Huang, Z. Deng, J. Tian and T. Liu, Synthesis and biological evaluation of salinomycin triazole analogues as anticancer agents, *Eur. J. Med. Chem*., 2017, **127**, 900–908. doi: 10.1016/j.ejmech.2016.10.067
43. K. Karrouchi, L. Chemlal, J. Taoufik, Y. Cherrah, S. Radi, M.El Abbes Faouzi and M. Ansar, Synthesis, antioxidant and analgesic activities of Schiff bases of 4-amino-1,2,4-triazole derivatives containing a pyrazole moiety, *Ann. Pharm. Fr*., 2016, **74**, no. 6, 431–438. doi: 10.1016/j.pharma.2016.03.005
44. O.A. Goncharova, A.Y. Luchkin, N.N. Andreev, N.P. Andreeva and S.S. Vesely, Triazole derivatives as chamber inhibitors of copper corrosion, *Int. J. Corros. Scale Inhib*., 2018, **7**, no. 4, 657–672. doi: 10.17675/2305-6894-2018-7-4-12

45. K.F. Khaled, Molecular simulation, quantum chemical calculations and electrochemical studies for inhibition of mild steel by triazoles, *Electrochim. Acta*, 2008, **53**, no. 9, 3484–3492. doi: 10.1016/j.electacta.2007.12.030
46. S. Maddila, R. Pagadala and S. Jonnalagadda, 1,2,4-Triazoles: A Review of Synthetic Approaches and the Biological Activity, *Lett. Org. Chem*., 2013, **10**, no. 10, 693–714. doi: 10.2174/15701786101010131126115448
47. L.P. Guan, Q.H. Jin, G.R. Tian, K.Y. Chai and Z.S. Quan, Synthesis of some quinoline2(1*H*)-one and 1,2,4-triazolo[4,3-a] quinoline derivatives as potent anticonvulsants, *J. Pharm. Pharm. Sci*., 2007, **10**, no. 3, 254–262.
48. R. Gujjar, A. Marwaha, F.El Mazouni, J.K. White, K.L. White, S. Creason, D.M. Shackleford, J. Baldwin, W.N. Charman, F.S. Buckner, S. Charman, P.K. Rathod and M.A. Phillips, Identification of a metabolically stable triazolopyrimidine-based dihydroorotate dehydrogenase inhibitor with antimalarial activity in mice, *J. Med. Chem*., 2009, **52**, no. 7, 1864–1872. doi: 10.1021/jm801343r
49. B. Hammouti, A. Zarrouk, S.S. Al-Deyab and I. Warad, Temperature Effect, Activation Energies and Thermodynamics of Adsorption of ethyl 2-(4-(2-ethoxy-2-oxoethyl)-2-p-Tolylquinoxalin-1(4H)-yl) Acetate on Cu in HNO_3, *Orient. J. Chem*., 2011, **27**, no. 1, 23–31.
50. E.A. Noor and A.H. Al-Moubaraki, Thermodynamic study of metal corrosion and inhibitor adsorption processes in mild steel/1-methyl-4[4'-(-X)-styryl pyridinium iodides/hydrochloric acid systems, *Mater. Chem. Phys*., 2008, **110**, no. 1, 145–154. doi: 10.1016/j.matchemphys.2008.01.028
51. O. Benali, L. Larabi, M. Traisnel, L. Gengembre and Y. Harek, Electrochemical, theoretical and XPS studies of 2-mercapto-1-methylimidazole adsorption on carbon steel in 1 M $HClO_4$, *Appl. Surf. Sci*., 2007, **253**, no. 14, 6130–6139. doi: 10.1016/j.apsusc.2007.01.075
52. P. Muthukrishnan, B. Jeyaprabha and P. Prakash, Adsorption and corrosion inhibiting behavior of *Lannea coromandelica* leaf extract on mild steel corrosion, *Arabian J. Chem*., 2017, **10**, S2343–S2354. doi: 10.1016/j.arabjc.2013.08.011
53. M. Hadizadeh, L. Yang, G. Fang, Z. Qiu and Z. Li, The mobility and solvation structure of a hydroxyl radical in a water nanodroplet: a Born–Oppenheimer molecular dynamics study, *Phys. Chem. Chem. Phys*., 2021, **23**, 14628–14635. doi: 10.1039/D1CP01830B
54. M. Hadizadeh and M. Hamadanian, Adsorption of toxic gases by an open nanocone coupled with an iron atom, *Bulg. Chem. Commun*., 2014, **46**, no. 3, 576–579.
55. O.A. Goncharova, A.Yu. Luchkin, Yu.I. Kuznetsov, N.N. Andreev, N.P. Andreeva and S.S. Vesely, Octadecylamine, 1,2,3-benzotriazole and a mixture thereof as chamber inhibitors of steel corrosion, *Int. J. Corros. Scale Inhib*., 2018, **7**, no. 2, 203–212. doi: 10.17675/2305-6894-2018-7-2-7
56. Ya.G. Avdeev, D.S. Kuznetsov, M.V. Tyurina and M.A. Chekulaev, Protection of nickel-chromium steel in sulfuric acid solution by a substituted triazole, *Int. J. Corros. Scale Inhib*., 2015, **4**, no. 2, 146–161. doi: 10.17675/2305-6894-2015-4-1-146-161

57. I.A. Arkhipushkin, Yu.E. Pronin, S.S. Vesely and L.P. Kazansky, Electrochemical and XPS study of 2-mercaptobenzothiazole nanolayers on zinc and copper surface, *Int. J. Corros. Scale Inhib.*, 2014, **3**, no. 2, 78–88. doi: 10.17675/2305-6894-2014-3-2-078-088
58. V.A. Trapeznikov, I.N. Shabanova, A.V. Kholzakov and A.G. Ponomaryov, Studies of transition metal melts by X-ray electron magnetic spectrometer, *J. Electron Spectrosc. Relat. Phenom.*, 2004, **137–140**, 383–385. doi: 10.1016/j.elspec.2004.02.115
59. I.N. Shabanova, R.A. Nurullina, V.A. Trapeznikov and J.G. Manakov, Electronic magnet spectrometer, RU Patent 2338295 C1, 2008, IPC H01J49/48 (in Russian).
60. N.A. Gladkikh, M.A. Maleeva, L.B. Maksaeva, M.A. Petrunin, A.A. Rybkina, T.A. Yurasova, A.I. Marshakov and R.Kh. Zalavutdinov, Localized dissolution of carbon steel used for pipelines under constant cathodic polarization conditions. Initial stages of defect formation, *Int. J. Corros. Scale Inhib.*, 2018, **7**, no. 4, 683–696. doi: 10.17675/2305-6894-2018-7-4-14
61. O.Yu. Grafov, L.P. Kazansky, S.V. Dubinskaya and Yu.I. Kuznetsov, Adsorption of depocolin and inhibition of copper dissolution in aqueous solutions, *Int. J. Corros. Scale Inhib.*, 2019, **8**, no. 3, 549–559. doi: 10.17675/2305-6894-2019-8-3-6
62. K.F. Khaled, Molecular simulation, quantum chemical calculations and electrochemical studies for inhibition of mild steel by triazoles, *Electrochim. Acta*, 2008, **53**, no. 9, 3484–3492. doi: 10.1016/j.electacta.2007.12.030
63. R. Haldhar, D. Prasad, A. Saxena and P. Singh, *Valeriana Wallichii* Root Extract as a Green & Sustainable Corrosion Inhibitor for Mild Steel in Acidic Environments: Experimental and Theoretical, *Mater. Chem. Front.*, 2018, **2**, 1225–1237. doi: 10.1039/C8QM00120K
64. L.O. Olasunkanmi, I.B. Obot, M.M. Kabanda and E.E. Ebenso, Some quinoxalin-6-yl derivatives as corrosion inhibitors for mild steel in hydrochloric acid: Experimental and theoretical studies, *J. Phys. Chem. C*, 2015, **119**, no. 28, 16004–16019. doi: 10.1021/acs.jpcc.5b03285
65. M. Stern and A.L. Geary, Electrochemical polarization, I. theoretical analysis of the shape of polarisation curves, *J. Electrochem. Soc.*, 1957, **104**, no. 1, 56–63. doi: 10.1149/1.2428496
66. M.A. Amin, M.A. Ahmed, H.A. Arida, F. Kandemirli, M. Saracoglu, T. Arslan and M.A. Basaran, Monitoring corrosion and corrosion control of iron in HCl by non-ionic surfactants of the TRITON-X series – part III. Immersion time effects and theoretical studies, *Corros. Sci.*, 2011, **53**, no. 5, 1895–1909. doi: 10.1016/j.corsci.2011.02.007
67. N.O. Eddy and B.I. Ita, QSAR, DFT and quantum chemical studies on the inhibition potentials of some carbozones for the corrosion of mild steel in HCl, *J. Mol. Model.*, 2011, **17**, no. 2, 359–376. doi: 10.1007/s00894-010-0731-7
68. S. Zhang, W. Lei, M. Xia and F. Wang, QSAR study on *N*-containing corrosion inhibitors: quantum chemical approach assisted by topological index, *J. Mol. Struct.: THEOCHEM*, 2005, **732**, no. 1–3, 173–182. doi: 10.1016/j.theochem.2005.02.091

69. O. Tapia, Solvent effect theories: Quantum and classical formalisms and their applications in chemistry and biochemistry, *J. Math. Chem*., 1992, **10**, no. 1, 139–181. doi: 10.1007/BF01169173
70. B.I.A. Simkin and I.I. Sheĭkhet, Quantum chemical and statistical theory of solutions: a computational approach, Ellis Horwood, London, 1995.
71. J. Tomasi and M. Persico, Molecular interactions in solution: an overview of methods based on continuous distributions of the solvent, *Chem. Rev*., 1994, **94**, no. 7, 2027–2094. doi: 10.1021/cr00031a013
72. M. Cossi, V. Barone, R. Cammi and J. Tomasi, Ab initio study of solvated molecules: a new implementation of the polarizable continuum model, *Chem. Phys. Lett*., 1996, **255**, no. 4–6, 327–335. doi: 10.1016/0009-2614(96)00349-1
73. V. Barone, M. Cossi and J. Tomasi, Geometry optimization of molecular structures in solution by the polarizable continuum model, *J. Comput. Chem*., 1998, **19**, no. 4, 404–417.
74. H. El Ashry, A. El Nemr, S. Essawy and S. Ragab, Corrosion inhibitors part IV: Quantum chemical studies on the corrosion inhibition of steel in acidic medium by some aniline derivatives, *J. Phys. Chem*., 2006, **1**, 41–55.
75. I. Lukovits, A. Shaban and E. Kálmán, Corrosion inhibitors: quantitative structure–activity relationships, *Russ. J. Electrochem*., 2003, **39**, no. 2, 177–181. doi: 10.1023/A:1022313126231
76. M. Lebrini, F. Bentiss, H. Vezin and M. Lagrenée, Inhibiting effects of some oxadiazole derivatives on the corrosion of mild steel in perchloric acid solution, *Appl. Surf. Sci*., 2005, **252**, no. 4, 950–958. doi: 10.1016/j.apsusc.2005.01.160
77. M. Lebrini, M. Lagrenee, H. Vezin, L. Gengembre and F. Bentiss, Electrochemical and quantum chemical studies of new thiadiazole derivatives adsorption on mild steel in normal hydrochloric acid medium, *Corros. Sci*., 2005, **47**, no. 2, 485–505. doi: 10.1016/j.corsci.2004.06.001
78. F. Bentiss, M. Traisnel, H. Vezin, H. Hildebrand and M. Lagrenee, 2,5-Bis(4-dimethylaminophenyl)-1,3,4-oxadiazole and 2,5-bis(4-dimethylaminophenyl)-1,3,4-thiadiazole as corrosion inhibitors for mild steel in acidic media, *Corros. Sci*., 2004, **46**, no. 11, 2781–2792. doi: 10.1016/j.corsci.2004.04.001
79. F. Bentiss, M. Lebrini, H. Vezin and M. Lagrenée, Experimental and theoretical study of 3-pyridyl-substituted 1,2,4-thiadiazole and 1,3,4-thiadiazole as corrosion inhibitors of mild steel in acidic media, *Mater. Chem. Phys*., 2004, **87**, no. 1, 18–23. doi: 10.1016/j.matchemphys.2004.05.040
80. F. Bentiss, M. Traisnel, H. Vezin and M. Lagrenée, Linear resistance model of the inhibition mechanism of steel in HCl by triazole and oxadiazole derivatives: structure–activity correlations, *Corros. Sci*., 2003, **45**, no. 2, 371–380. doi: 10.1016/S0010-938X(02)00102-6
81. F. Bentiss, M. Traisnel, N. Chaibi, B. Mernari, H. Vezin and M. Lagrenée, 2,5-Bis(nmethoxyphenyl)-1,3,4-oxadiazoles used as corrosion inhibitors in acidic media:

correlation between inhibition efficiency and chemical structure, *Corros. Sci*., 2002, **44**, no. 10, 2271–2289. doi: 10.1016/S0010-938X(02)00037-9
82. M. Lagrenee, B. Mernari, M. Bouanis, M. Traisnel and F. Bentiss, Study of the mechanism and inhibiting efficiency of 3,5-bis(4-methylthiophenyl)-4H-1,2,4-triazole on mild steel corrosion in acidic media, *Corros. Sci*., 2002, **44**, no. 3, 573–588. doi: 10.1016/S0010-938X(01)00075-0
83. M. Lagrenee, B. Mernari, N. Chaibi, M. Traisnel, H. Vezin and F. Bentiss, Investigation of the inhibitive effect of substituted oxadiazoles on the corrosion of mild steel in HCl medium, *Corros. Sci*., 2001, **43**, no. 5, 951–962. doi: 10.1016/S0010-938X(00)00076-7
84. A. Alija, D. Gashi, R. Plakaj, A. Omaj, V. Thaçi, A. Reka, S. Avdiaj and A. Berisha, A theoretical and experimental study of the adsorptive removal of hexavalent chromium ions using graphene oxide as an adsorbent, *Open Chem*., 2020, **18**, no. 1, 936–942. doi: 10.1515/chem-2020-0148
85. A. Klamt, The COSMO and COSMO-RS solvation models, *Wiley Interdiscip. Rev.: Comput. Mol. Sci*., 2018, **8**, no. 1, e1338. doi: 10.1002/wcms.1338
86. A. Berisha, Interactions between the aryldiazonium cations and graphene oxide: A DFT study, *J. Chem*., 2019, **2019**, 5126071. doi: 10.1155/2019/5126071
87. R. Hsissou, O. Dagdag, S. Abbout, F. Benhiba, M. Berradi, M. El Bouchti, A. Berisha, N. Hajjaji and A. Elharfi, Novel derivative epoxy resin TGETET as a corrosion inhibition of E24 carbon steel in 1.0 M HCl solution. Experimental and computational (DFT and MD simulations) methods, *J. Mol. Liq*., 2019, **284**, 182–192. doi: 10.1016/j.molliq.2019.03.180
88. O. Dagdag, R. Hsissou, A. El Harfi, A. Berisha, Z. Safi, C. Verma, E.E. Ebenso, M. Ebn Touhami and M. El Gouri, Fabrication of polymer based epoxy resin as effective anti-corrosive coating for steel: Computational modeling reinforced experimental studies, *Surf. Interfaces*, 2020, **18**, 100454. doi: 10.1016/j.surfin.2020.100454
89. H. Sun, Z. Jin, C. Yang, R.L.C. Akkermans, S.H. Robertson, N.A. Spenley, S. Miller and S.M. Todd, COMPASS II: extended coverage for polymer and drug-like molecule databases, *J. Mol. Model*., 2016, **22**, no. 47, 1–10. doi: 10.1007/s00894-016-2909-0
90. M. El Faydy, F. Benhiba, A. Berisha, Y. Kerroum, C. Jama, B. Lakhrissi, A. Guenbour, I. Warad and A. Zarrouk, An experimental-coupled empirical investigation on the corrosion inhibitory action of 7-alkyl-8-Hydroxyquinolines on C35E steel in HCl electrolyte, *J. Mol. Liq*., 2020, **317**, 113973. doi: 10.1016/j.molliq.2020.113973
91. S. El Arrouji, K. Karrouchi, A. Berisha, K.I. Alaoui, I. Warad, Z. Rais, S. Radi, M. Taleb, M. Ansar and A. Zarrouk, New pyrazole derivatives as effective corrosion inhibitors on steel-electrolyte interface in 1 M HCl: Electrochemical, surface morphological (SEM) and computational analysis, *Colloids Surf., A*, 2020, **604**, 125325. doi: 10.1016/j.colsurfa.2020.125325
92. M. Damej, A. Molhi, H. Lgaz, R. Hsissou, J. Aslam, M. Benmessaoud, N. Rezki, H.S. Lee and D.E. Lee, Performance and interaction mechanism of a new highly efficient benzimidazole-based epoxy resin for corrosion inhibition of carbon steel in HCl: A study

based on experimental and first-principles DFTB simulations, *J. Mol. Struct*., 2023, **1273**, 134232. doi :10.1016/j.molstruc.2022.134232

93. M. Damej, S. Kaya, B. El Ibrahimi, H.S. Lee, A. Molhi, G. Serdaroğlu, M. Benmessaoud, I.H. Ali, S. El Hajjaji and H. Lgaz, The corrosion inhibition and adsorption behavior of mercaptobenzimidazole and bis-mercaptobenzimidazole on carbon steel in 1.0 M HCl: Experimental and computational insights, *Surf. Interfaces*, 2021, **24**, 101095. doi: 10.1016/j.surfin.2021.101095
94. F. Bouhlal, A. Mazkour, H. Labjar, M. Benmessaoud, M. Serghini-Idrissi, M. El Mahi, S. El Hajjaji and N. Labjar, Combination effect of hydro-alcoholic extract of spent coffee grounds (HECG) and potassium Iodide (KI) on the C38 steel corrosion inhibition in 1 M HCl medium: Experimental design by response surface methodology, *Chem. Data Collect*., 2020, **29**, 100499. doi: 10.1016/j.cdc.2020.100499
95. M.E. Ansar, R. Hsissou, B.E. Ibrahimi, A.A. Addi, A. Molhi, M. Damej, S. El Hajjaji and M. Benmessaoud, Electrochemical and thermodynamic study of the inhibitory effect of triglycidyl ether tripropoxy triazine (TGETPT) on the corrosion of carbon steel E24 in 1 M hydrochloric acid medium, *Int. J. Corros. Scale Inhib*., 2023, **12**, no. 3, 1065–1087. doi: 10.17675/2305-6894-2023-12-3-16
96. H. Wu, H. Lei, Y.F. Chen and J. Qiao, Comparison on corrosion behaviour and mechanical properties of structural steel exposed between urban industrial atmosphere and laboratory simulated environment, *Constr. Build. Mater*., 2019, **211**, 228–243. doi: 10.1016/j.conbuildmat.2019.03.207
97. Yu.P. Vyshnevska and I.V. Brazhnyk, Corrosion prevention and control using in situ phase layers formation via application of the complexing-type inhibitors, *Appl. Res*., 2023, 1–9. doi. 10.1002/appl.202300027
98. A. Espinoza-Vázquez, F.J. Rodríguez-Gómez, I.K. Martínez-Cruz, D. Ángeles-Beltrán, G.E. Negrón-Silva, M. Palomar-Pardavé, L.L. Romero, D. Pérez-Martínez and A.M. Navarrete-López, Adsorption and corrosion inhibition behaviour of new theophylline–triazole-based derivatives for steel in acidic medium, *R. Soc. Open Sci.*, 2019, **6**, no. 3, 181738. doi: 10.1098/rsos.181738
99. H.H. Hassan, E. Abdelghani and M.A. Amin, Inhibition of mild steel corrosion in hydrochloric acid solution by triazole derivatives: Part I. Polarization and EIS studies, *Electrochim. Acta*, 2007, **52**, no. 22, 6359–6366. doi: 10.1016/j.electacta.2007.04.046
100. S. Ramesh and S.S. Rajeswari, Corrosion inhibition of mild steel in neutral aqueous solution by new triazole derivatives, *Electrochim. Acta*, 2004, **49**, no. 5, 811–820. doi: 10.1016/j.electacta.2003.09.035

♦ ♦ ♦